Supporting Information

Monopicolinate Cross-bridged Cyclam Combining Very Fast Complexation with Very High Stability and Inertness of its Copper(II) Complex

Luís M. P. Lima,[‡] *Zakaria Halime,*[†] *Ronan Marion,*[†] *Nathalie Camus,*[†] *Rita Delgado,**[,‡] *Carlos Platas-Iglesias,*[§] *and Raphaël Tripier* *[,†]

[‡]Instituto de Tecnologia Química e Biológica, Universidade Nova de Lisboa, Av. da República, 2780-157 Oeiras, Portugal. [†]Université de Bretagne Occidentale, UMR-CNRS 6521, UFR des Sciences et Techniques, 6 avenue Victor le Gorgeu, C.S. 93837, 29238 Brest Cedex 3, France. [§]Departamento de Química Fundamental, Universidade da Coruña, Campus da Zapateira, Rúa da Fraga 10, 15008 A Coruña, Spain.

Summary

Figure S1. "Ball and stick" view of [Cu(**cb-te1pa**)]$(ClO_4)_2$. Perchlorate anions and water molecules are omitted for clarity.

Table S1. Selected bond lengths (Å) and angles (º) of the metal coordination environments in [Cu(**cb-te1pa)**]$(ClO_4)_2$. See Figure 2 for labeling.

Figure S2. ^{1}H NMR titration of H**cb-te1pa** in D_2O solution, showing only the resonances arising from the pendant arm for simplicity.

Figure S3. Speciation diagrams of Cu^{2+} (left) and Zn^{2+} (right) in presence of H**cb-te1pa** at $C_{M^{2+}} = C_{\mathbf{Hcb\text{-}te1pa}} = 10^{-3}$ M.

Figure S4. UV and vis-NIR spectra of the copper(II) complex of H**cb-te1pa** in aqueous solution.

Figure S5. ^{1}H NMR (500 MHz) spectra at variable temperature (5, 15, 25, 40, 55 and 70 °C from bottom to top) of the [Zn(**cb-te1pa**)]$^+$ complex in D_2O at pD = 6.8.

Figure S6. ^{13}C NMR (125 MHz) spectra at variable temperature (5, 15, 25, 40, 55 and 70 °C from bottom to top) of the [Zn(**cb-te1pa**)]$^+$ complex in D_2O at pD = 6.8.

Figure S7. Time course of the copper(II) complexation by H**cb-te1pa** in equimolar amount at $C_{M^{2+}} = C_{\mathbf{Hcb\text{-}te1pa}} = 0.8$ mM) and pH = 5 in acetate buffer, as followed by the increasing complex absorbance band at 600 nm.

Figure S8. Arrhenius plot for the acid-assisted dissociation of the copper(II) complex of H**cb-te1pa** in 5 M HCl aqueous solutions.

Table S2. Optimized Cartesian coordinates obtained with DFT calculations for [Cu(**cb-te1pa**)]$^{2+}$.

Figure S9. ^{1}H NMR spectrum (298K, 300 MHz, $CDCl_3$) of compound **3**.

Figure S10. ^{13}C NMR spectrum (298K, 75 MHz, $CDCl_3$) of compound **3**.

Figure S11. ^{1}H NMR spectrum (298K, 300 MHz, D_2O) of compound H**cb-te1pa**

Figure S12. ^{13}C NMR spectrum (298K, 75 MHz, D_2O) of compound H**cb-te1pa.**

Figure S13. Elementary analysis of compound **3** and **Hcb-te1pa**

Figure S14. HR-MS spectra the copper(II) complex of **cb-te1pa.**

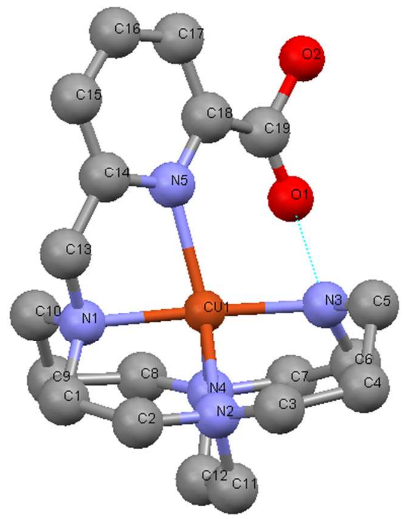

Figure S1. "Ball and stick" view of [Cu(**cb-te1pa**)](ClO_4)$_2$. Perchlorate anions and water molecules are omitted for clarity.

Table S1. Selected bond lengths (Å) and angles (º) of the metal coordination environments in [Cu(**cb-te1pa)**](ClO_4)$_2$. See Figure S1 for labeling.

Cu(1)–N(1)	2.010(6)	N(3)–Cu(1)–N(5)	102.1(2)
Cu(1)–N(2)	2.138(6)	N(5)–Cu(1)–N(5)	80.4(2)
Cu(1)–N(3)	1.966(6)	N(4)–Cu(1)–N(5)	127.7(2)
Cu(1)–N(4)	2.108(6)	N(3)–Cu(1)–N(2)	90.7(2)
Cu(1)–N(5)	2.113(6)	N(1)–Cu(1)–N(2)	85.1(2)
N(1)–Cu(1)–N(3)	175.4(3)	N(4)–Cu(1)–N(2)	86.2(2)
N(3)–Cu(1)–N(4)	87.4(2)	N(5)–Cu(1)–N(2)	143.7(2)
N(1)–Cu(1)–N(4)	94.1(2)		

X-ray diffraction determination of [Cu(**cb-te1pa**)](ClO_4)$_2$:

Single crystals of the complex of H**cb-te1pa** with Cu^{2+} were obtained by slow evaporation of a concentrated aqueous solution at neutral pH. Crystals were found to be composed of the [Cu(**cb-te1pa**)]$^{2+}$ cation, two perchlorate anions, and water molecules. A view of the structure of the complex cation is shown in Figure S1, while bond distances and angles of the metal coordination environment are given in Table S1.

The metal ion in [Cu(**cb-te1pa**)]$^{2+}$ is five coordinated, being directly bound to the four nitrogen atoms of the macrocyclic unit and the nitrogen atom of the pyridyl group. The distance between the metal atom and the oxygen atom of the carboxylic group O(1) [3.16 Å] is too long to be considered as a bond distance. The coordination polyhedron around the copper center can be defined as a trigonal bipyramid, in which the equatorial plane is defined by the N atoms of the cyclam fragment N2 and N4, the nitrogen atom of the pyridyl unit N5 and the metal ion, and the apical positions are defined by donor atoms N1 and N3. Alternatively, the coordination polyhedron may be defined as square pyramidal, where the basal plane is formed by N1, N2, N3 and N5, and the apical position is defined by N4. The index of trigonality τ is calculated to be 0.53, which points to a distorted coordination polyhedron that is halfway between the two ideal geometries (τ = 0 for a perfect square-pyramidal geometry and τ = 1 for an ideal trigonal-bipyramidal geometry).[1]

The cyclam unit presents a *cis*-V-folded coordination configuration[2] that provides four convergent nitrogen donor atoms for Cu^{2+} coordination. The bicyclo[6.6.2] ligand backbone shows a [2323]/[2323] conformation,[3] as often observed in structures of Cu^{2+} complexes of cross-bridged cyclam derivatives. Interestingly, the diprotonated form of the ligand adopts the same conformation. An intramolecular hydrogen bonding interaction exists between the NH group of the macrocyclic fragment and one of the oxygen atoms of the carboxylate function (N(3)···O(1) 2.808(7) Å, N(3)-H(3)···O(1) 2.16 Å, N(3)-H(3)···O(1) 126.0º; N(3)···O(1) 2.814(3) Å, N(3)-H(3)···O(1) 2.16 Å, N(3)-H(3)···O(1) 126.9º), which results in the formation of a macrotricyclic-like structure due to the formation of a third pseudomacrocycle.

In $[Cu(\mathbf{cb\text{-}te1pa})]^{+}$ the donor atom of the macrocyclic fragment N3 provides the strongest interaction with the copper center, with bond distance of 1.97 Å, the other Cu–N distances in the range 2.01–2.14 Å. These bond distances are shorter than those observed for $[Cu(\mathbf{te1pa})]^{+}$ (2.00–2.35 Å) related five-coordinated copper(II) complexes with cyclam-based ligand lacking the cross-bridge unit,[4] which points to a particularly strong interaction of the **cb-te1pa**$^{-}$ ligand with Cu^{2+}.

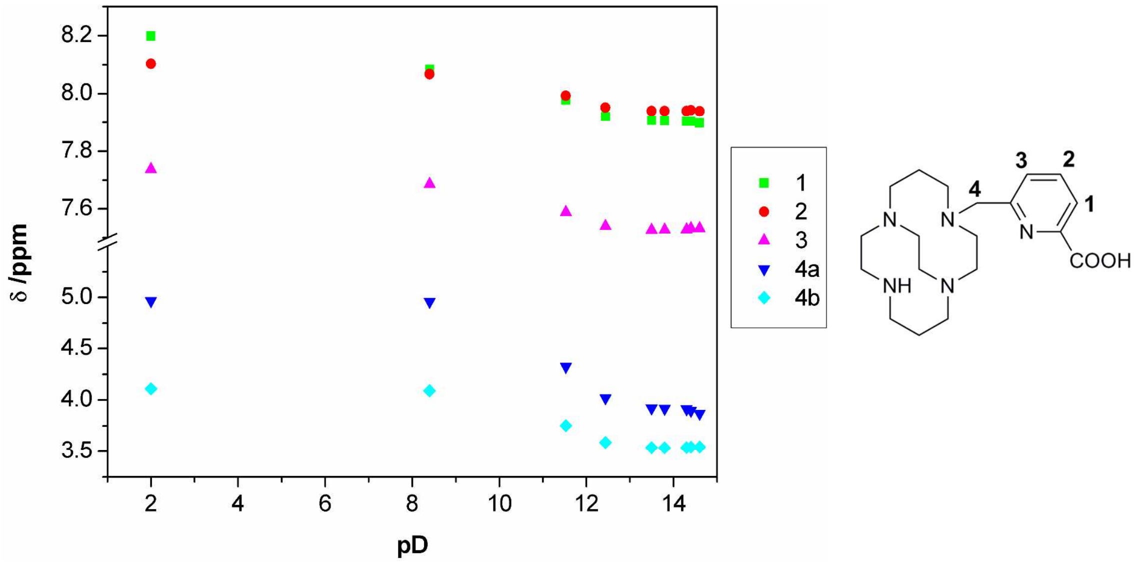

Figure S2. ^{1}H NMR titration of H**cb-te1pa** in D_2O solution and the corresponding resonance labeling, showing only the resonances arising from the pendant arm for simplicity. Aromatic protons are labeled 1, 2 and 3, while non-equivalent methylene protons are labeled 4a and 4b.

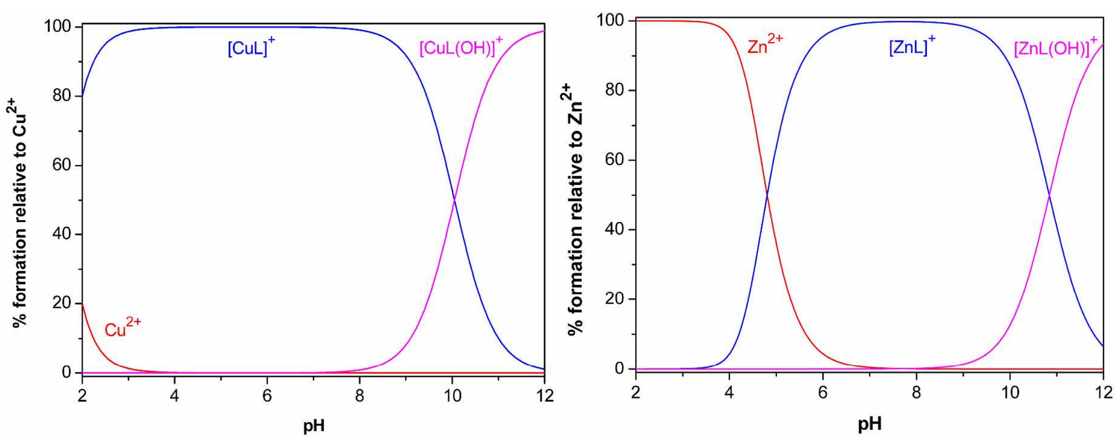

Figure S3. Speciation diagrams of H**cb-te1pa** ligand in presence of Cu^{2+} (left) and Zn^{2+}. (right) in aqueous solution at $C_{M^{2+}} = C_{H\mathbf{cb\text{-}te1pa}} = 10^{-3}$ M.

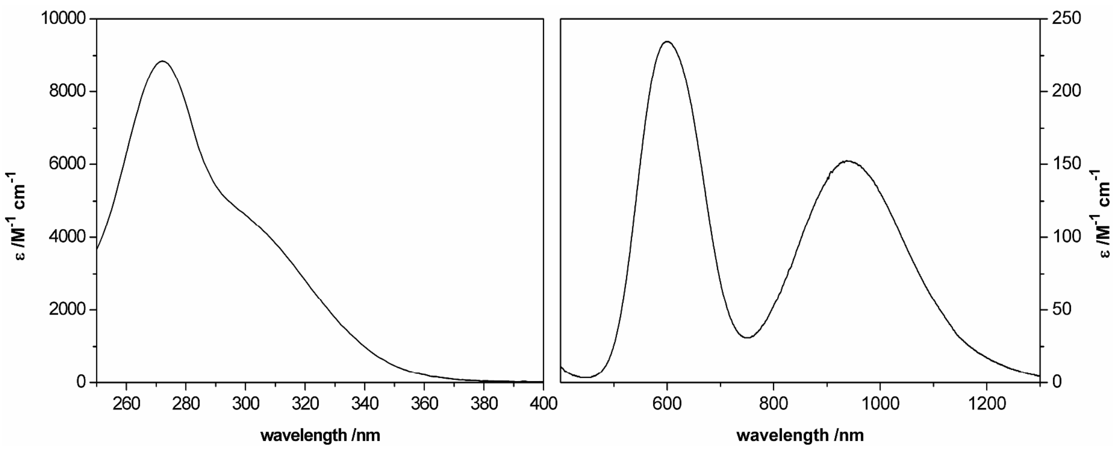

Figure S4. UV (left) and vis-NIR (right) spectra of the copper(II) complex of H**cb-te1pa** in aqueous solution at pH = 7.5 and RT.

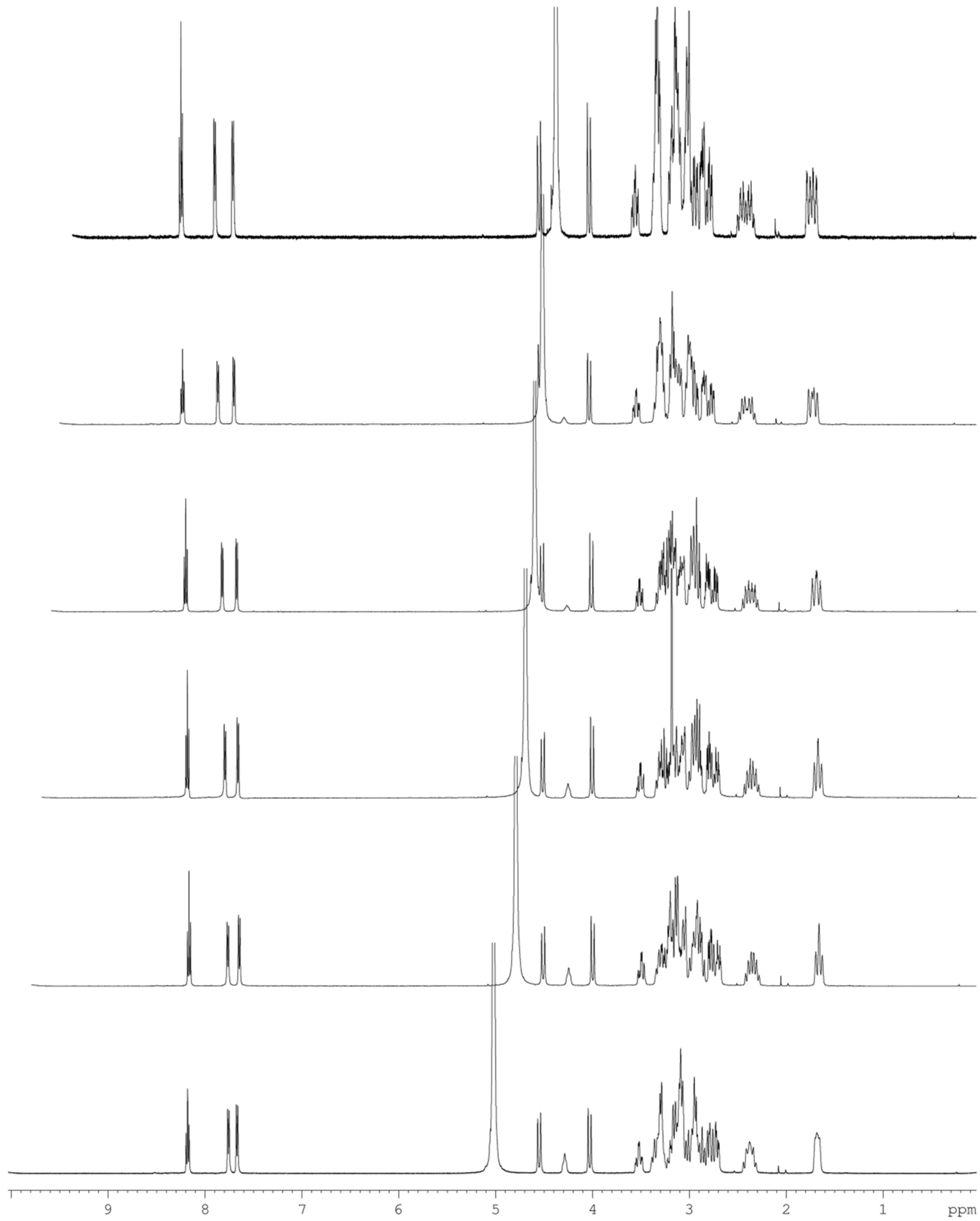

Figure S5. ^{1}H NMR (500 MHz) spectra at variable temperature (5, 15, 25, 40, 55 and 70 °C from bottom to top) of the $[Zn($**cb-te1pa**$)]^{+}$ complex in D_2O at pD = 6.8.

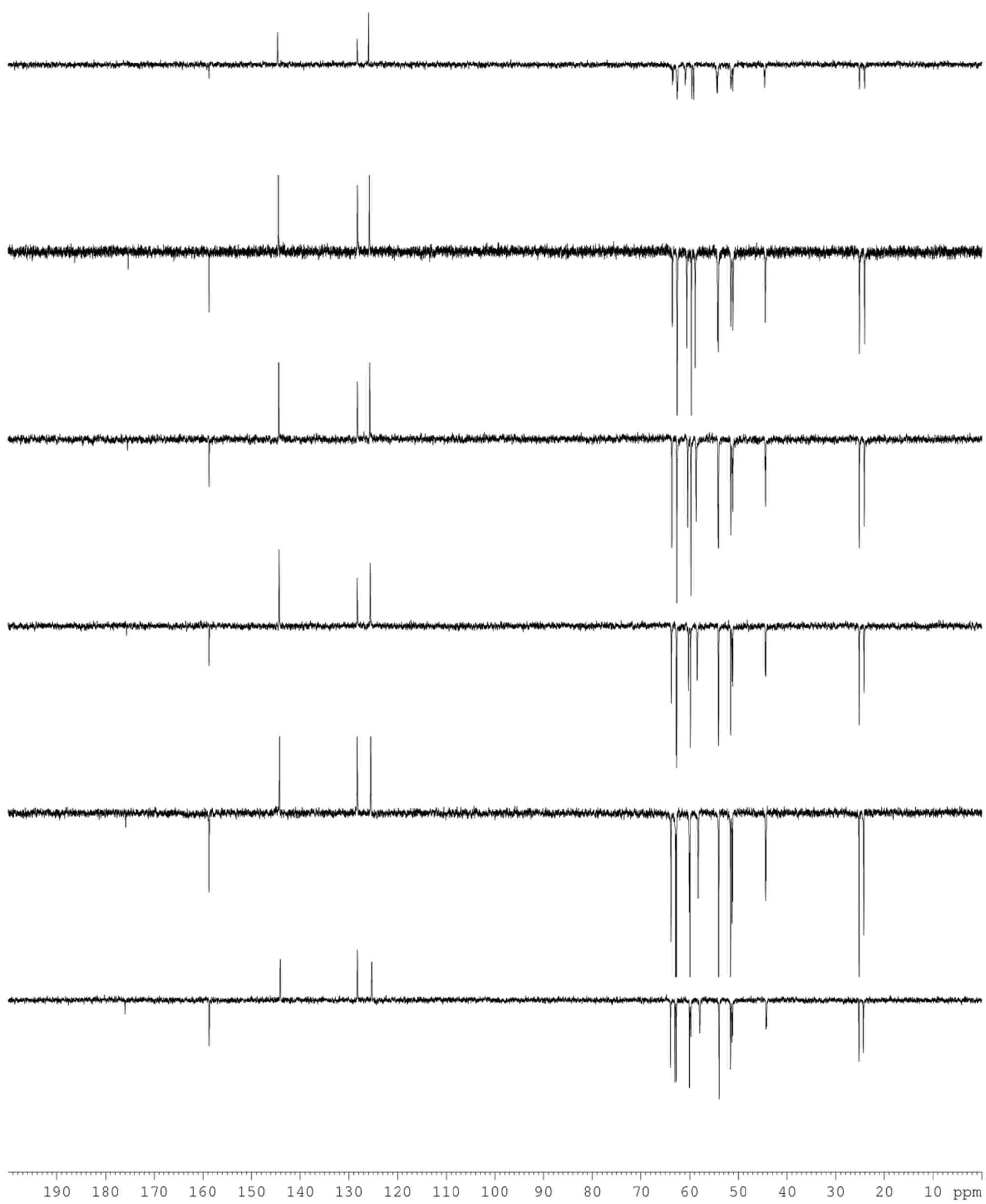

Figure S6. ^{13}C NMR (125 MHz) spectra at variable temperature (5, 15, 25, 40, 55 and 70 °C from bottom to top) of the $[Zn($**cb-te1pa**$)]^{+}$ complex in D_2O at pD = 6.8.

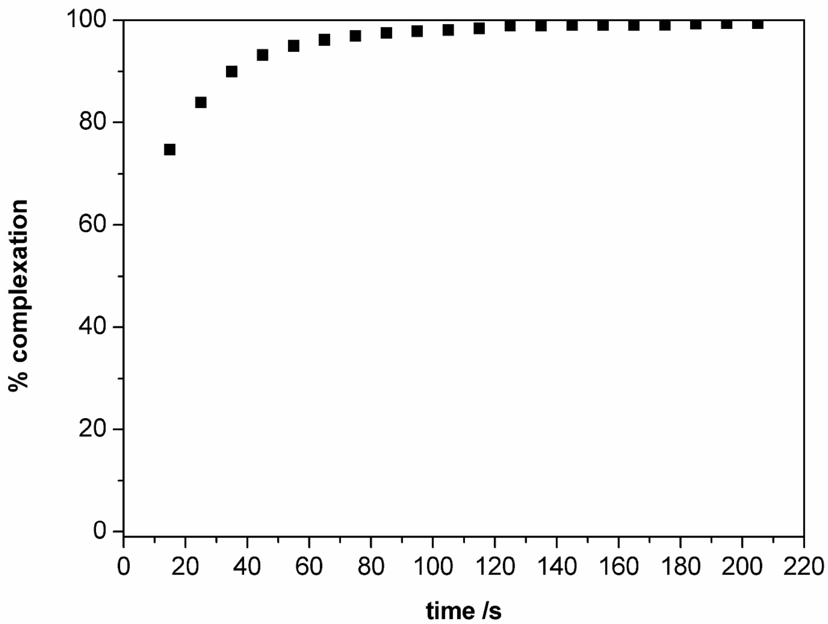

Figure S7. Time course of the copper(II) complexation by H**cb-te1pa** in equimolar amount at $C_{M^{2+}}$ = $C_{\mathbf{Hcb\text{-}te1pa}}$ = 0.8 mM) and pH = 5 in acetate buffer, as followed by the increasing complex absorbance band at 600 nm.

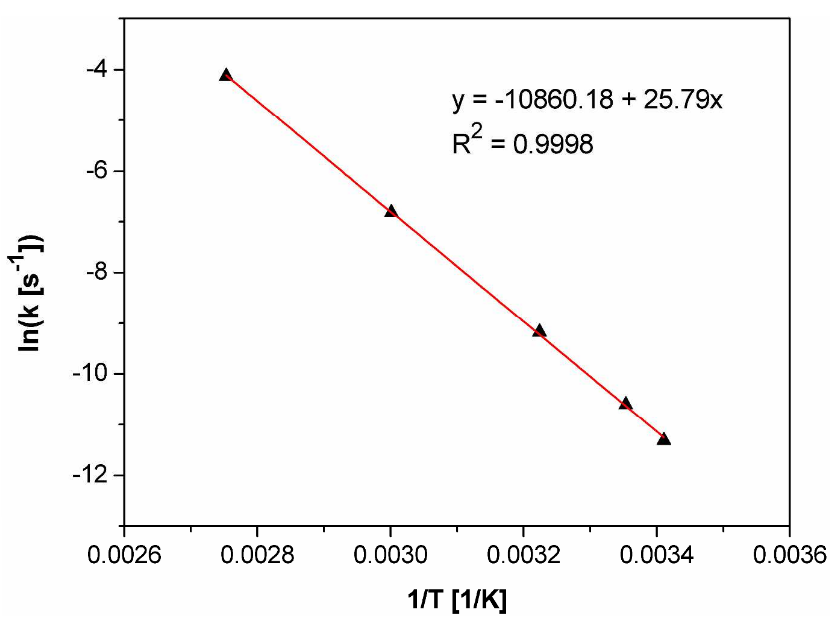

Figure S8. Arrhenius plot for the acid-assisted dissociation of the copper(II) complex of H**cb-te1pa** in 5 M HCl aqueous solutions.

Table S2. Optimized Cartesian coordinates obtained with DFT calculations for [Cu(**cb-te1pa**)]$^{+}$.

[Cu(**cb-te1pa**)]$^{2+}$, TPSSh/TZVP (0 imaginary frequencies)

C	-1.52687000	-2.50949100	-0.73583200
H	-2.26255100	-2.60581700	0.05621900
H	-1.37901900	-3.50713800	-1.16180800
C	-2.01474300	-1.54906200	-1.80670900
H	-1.35069700	-1.57445200	-2.67166600
H	-3.00888300	-1.85671500	-2.15145100
C	-2.03556300	0.77575400	-2.48608900
H	-1.19836600	0.46360500	-3.11370900
H	-2.95738500	0.62638000	-3.06279400
C	-1.88743400	2.26091300	-2.16268400
H	-2.76927300	2.64462200	-1.64390600
H	-1.87604600	2.78120100	-3.12481900
C	-0.61179600	2.65821400	-1.42360800
H	0.26537000	2.35936900	-2.00200600
H	-0.58613700	3.74913500	-1.32096700
C	-1.49087200	2.47281100	0.90787400
H	-1.24849100	3.47478000	1.27524400
H	-2.46718600	2.53495800	0.43284200
C	-1.50302000	1.49537900	2.07247000
H	-2.31607600	1.74083400	2.76629800
H	-0.55550000	1.57045800	2.60673500
C	-1.21905800	-0.83629100	2.69341300
H	-1.94984200	-0.78198200	3.51104900
H	-0.26826700	-0.46098700	3.07655200
C	-1.05158100	-2.29793500	2.28116700
H	-2.01114000	-2.75045100	2.02085400
H	-0.72775700	-2.83070500	3.18017500
C	0.00314100	-2.59925400	1.21824300
H	0.97346200	-2.21618000	1.54072700
H	0.09373700	-3.68616900	1.10640200
C	-3.20154900	0.10690700	-0.41556500
H	-4.06673600	-0.47022300	-0.76110900
H	-3.46790000	1.15418400	-0.51950800
C	-2.97678500	-0.22494000	1.07637100
H	-3.73591900	0.31296500	1.65618800
H	-3.15558300	-1.28408400	1.24357900
C	0.87652900	-2.33421600	-1.03993700
H	0.56497300	-2.11594400	-2.06389700
H	1.11350300	-3.40155500	-0.98661200
C	2.08809500	-1.50860500	-0.71251200
C	3.35834800	-2.02020100	-0.94653700
H	3.46852100	-3.03138700	-1.31781300

C	4.46037200	-1.21567800	-0.69565000
H	5.46511800	-1.58094600	-0.87225000
C	4.24294900	0.06201800	-0.20401000
H	5.05846100	0.73795600	0.01177800
C	2.94524800	0.50616100	0.04797600
C	2.79525100	1.89191200	0.69237200
N	-0.25521800	-2.01428300	-0.13580600
N	-2.03899100	-0.14835200	-1.30976900
N	-0.47604300	2.03779800	-0.08511300
N	-1.62185700	0.09055400	1.59801400
N	1.86789900	-0.26998200	-0.21987400
O	3.72745100	2.69315000	0.47889700
Cu	-0.27087700	0.03003200	-0.07515300
O	1.76420000	2.08031800	1.40108200
H	0.44332100	2.26908800	0.33260100

E(UTPSSh) = -2807.206889 Hartree
Zero-point correction = 0.495427
Thermal correction to Energy = 0.519007
Thermal correction to Enthalpy = 0.519951
Thermal correction to Gibbs Free Energy = 0.444436
Sum of electronic and zero-point Energies = -2806.711462
Sum of electronic and thermal Energies = -2806.687882
Sum of electronic and thermal Enthalpies = -2806.686938
Sum of electronic and thermal Free Energies = -2806.762453

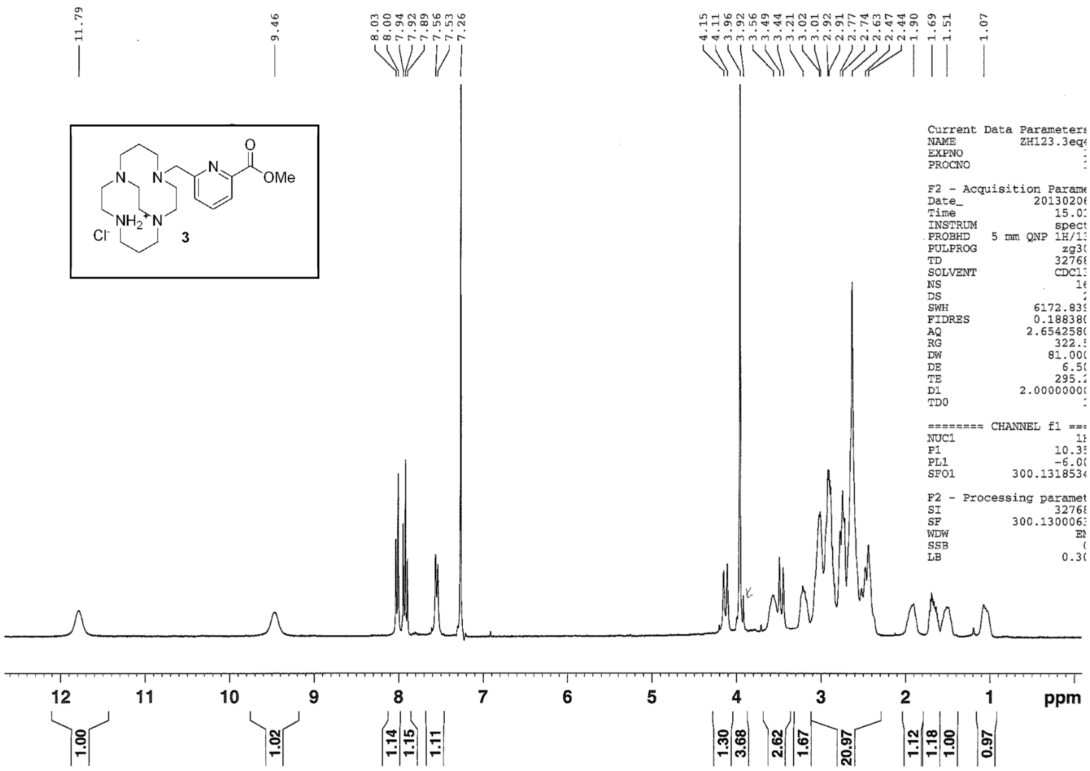

Figure S9. ^{1}H NMR spectrum (298K, 300 MHz, $CDCl_3$) of compound **3**.

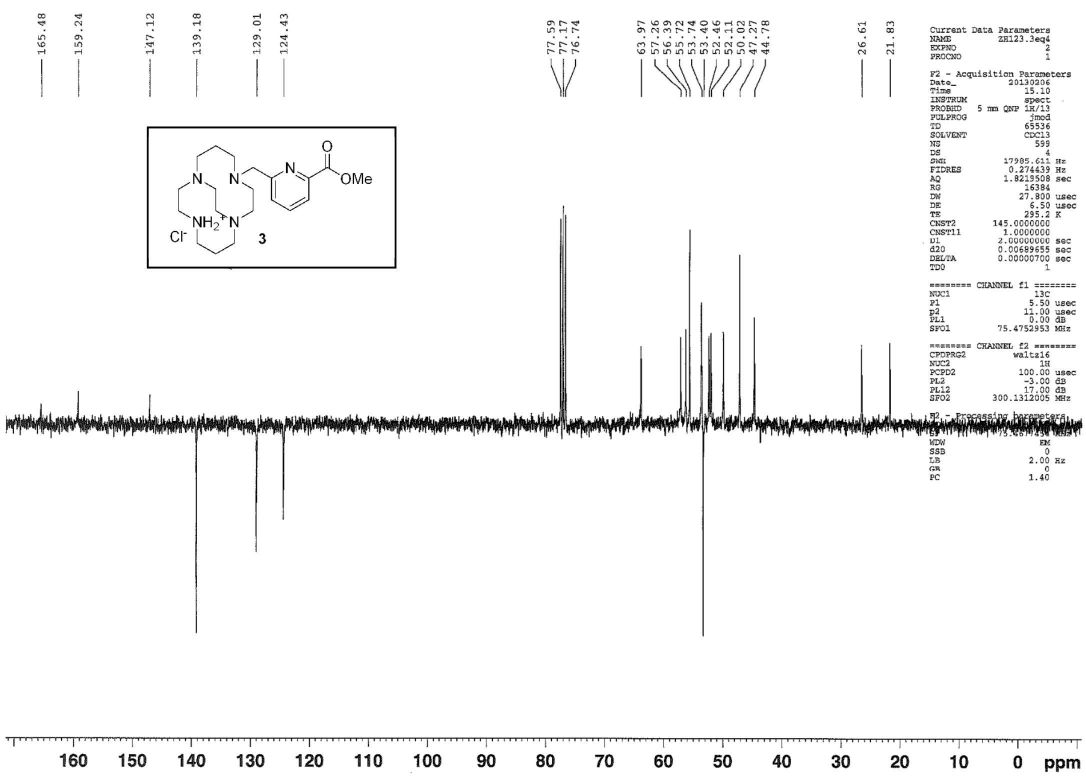

Figure S10. ^{13}C NMR spectrum (298K, 75 MHz, $CDCl_3$) of compound **3**.

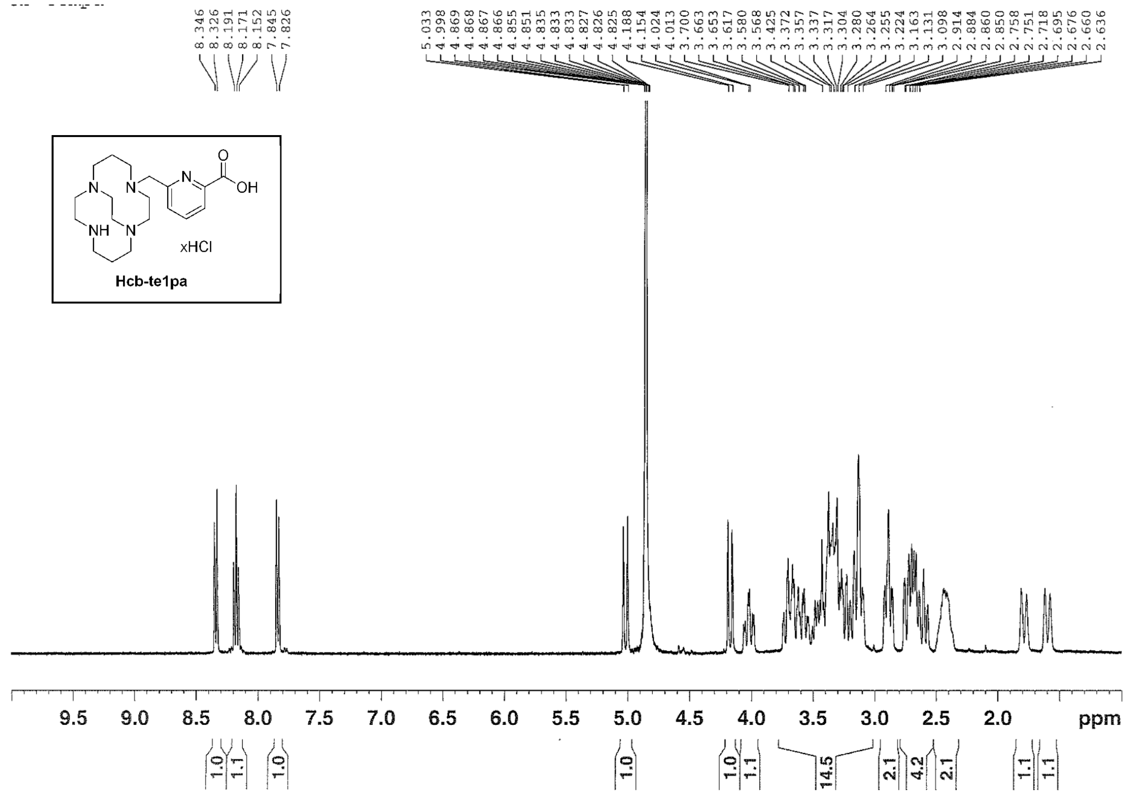

Figure S11. ^{1}H NMR spectrum (298K, 300 MHz, D_2O) of compound H**cb-te1pa**

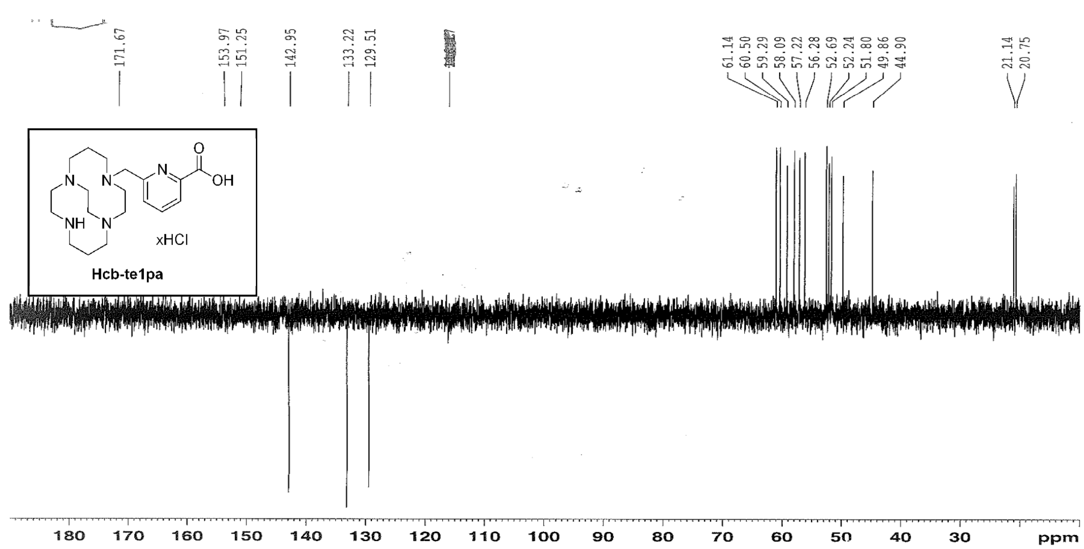

Figure S12. ^{13}C NMR spectrum (298K, 75 MHz, D_2O) of compound H**cb-te1pa.**

INSTITUT DES SCIENCES ANALYTIQUES

SERVICE CENTRAL D'ANALYSE

Villeurbanne le : 18/07/2013

Renseignements :
Bureau des Analyses
de 8h - 12h et 13h - 16h30
Tél : 04.37.42.36.36
Fax : 04.37.42.36.37
Mèl : bda@sca.cnrs.fr

CNRS UMR6521
CHIMIE, ELECTROCHIMIE MOLECULAIRES
ET CHIMIE ANALYTIQUE
M. TRIPIER
UNIVERSITE DE BRETAGNE OCCIDENTALE
DE BREST
UFR SCIENCES ET TECHNIQUES BAT C
6 AV VICTOR LE GORGEU - CS 93837
29238 BREST Cedex 3

Bulletin d'analyses BUL13/1565-1

Veuillez trouver ci-après, les résultats des analyses effectuées sur les échantillons que vous nous avez envoyés.

Bon de commande :	L04946/94.4.2013	**Du**	15/05/2013

Référence	ZH146	Date de réception	22/05/13	N° SCA	13/04541

C	53.62 %						
H	8.69 %						
N	15.35 %						

Remarques :

Référence	ZH164	Date de réception	22/05/13	N° SCA	13/04542

C	36.79 %						
H	7.22 %						
N	10.93 %						

Remarques :

ZH 146: compound **3**: ($C_{20}H_{33}N_5O_2 \cdot HCl \cdot 2H_2O$)

ZH 164: compound **Hcb-te1pa** ($C_{19}H_{31}N_5O_2 \cdot 5HCl \cdot 4.5H_2O$)

Responsable scientifique

1 / 1

Figure S13. Elementary analysis of compound **3** and **Hcb-te1pa**

Fédération de Recherche Physique et Chimie du Vivant (FR2708 : CBM/ICOA)
Plate-forme de Spectrométrie de Masse Haute Résolution

HRMS

Analysis Info

Sample Name	**ZH-TMPACu**	Acquisition Date	19/03/2014 13:41:29
Analysis Name	X013213CYC.d	Laboratory	
Method	Positif.m	Instrument / Ser#	maXis 255552.00086

Acquisition Parameter

Source Type	ESI	Ion Polarity	Positive	Set Nebulizer	0.6 Bar
Focus	Not active	Set Capillary	4500 V	Set Dry Heater	200 °C
Scan Begin	50 m/z	Set End Plate Offset	-500 V	Set Dry Gas	7.0 l/min
Scan End	3000 m/z	Set Collision Cell RF	1000.0 Vpp	Set Divert Valve	Waste

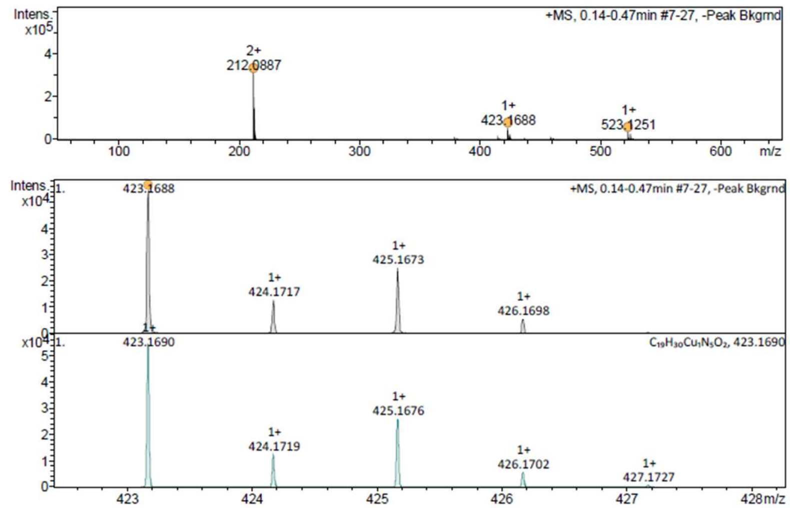

Meas. m/z	z	#	Ion Formula	m/z	err [ppm]	mSigma	rdb	e⁻ Conf
212.088712	2+	1	C19H31CuN5O2	212.088138	-2.7	6.3	6.5	odd
423.168836	1+	1	C19H30CuN5O2	423.168999	-0.4	9.2	7.0	odd
523.125126	1+	1	C19H31ClCuN5O6	523.125335	-0.4	12.2	6.0	odd
	1+	2	C18H25ClCuN12O	523.125330	0.4	14.8	11.5	even
	1+	3	C15H31Cu2N11O2	523.124866	0.5	53.7	5.0	odd
	1+	4	C16H37Cu2N4O7	523.124871	0.5	57.7	-0.5	even
	1+	5	C33H29ClCu	523.124828	-0.6	74.2	18.5	even

Figure S14. HR-MS spectra the copper(II) complex of **cb-te1pa.**

References

(1) Addison, A. W.; Nageswara-Rao, T.; Reedijk, J.; van Rijn, J.; Verschoor, G. C. *J. Chem. Soc., Dalton Trans.* **1984**, 1349–1356.

(2) Liang, X.; Sadler, P. J. *Chem. Soc. Rev.* **2004**, *33*, 246–266.

(3) Dale, J. *Acta Chem. Scand.* **1973**, *27*, 1115–1129.

(4) El Ghachtouli, S.; Cadiou, C.; Dechamps-Olivier, I.; Chuburu, F.; Aplincourt, M.; Roisnel, T. *Eur. J. Inorg. Chem.* **2006**, 3472–3481.